Supporting Information

CO Adsorption Site Preference on Platinum:

Charge Is the Essence

G.T. Kasun Kalhara Gunasooriya,[†] and Mark Saeys[*,†]

Laboratory for Chemical Technology, Ghent University, Technologiepark 914, 9052 Gent,

Belgium

Corresponding Author

*E−mail address: mark.saeys@ugent.be

Tel no.: +32 (0)9 331 1754

Table of Contents

Table S6. Change in the occupancy of various NBOs for CO adsorption at the top and the bridge site as a function of the charge of the surface Pt atoms. Calculations were done for a low CO coverage, with the vdW−DF functional and for a 5−layer $p(3\times3)$ Pt(111) slab.

Table S7. Effect of the surface Pt charge on the low coverage CO adsorption energy for the PBE functional and a 5−layer $p(3\times3)$ Pt(111) slab.

Table S8. vdW−DF frequencies of adsorbed CO for different configurations and coverages on Pt(111).

4. References

1. Computational methods

CO adsorption on Pt(111) was studied using periodic density functional theory with the vdW−DF,[1−2] PBE,[3] BEEF−vdW[4] and HSE06[5] functionals, a plane−wave basis set with a cut−off kinetic energy of 450 eV, and the projector−augmented wave method as implemented in the Vienna Ab−initio Simulation Package (VASP).[6−7] The Pt(111) surface was modelled as a five−layer slab using $p(3\times3)$ (for low coverage) and $c(4\times2)$ (for high coverage) unit cells. The bottom two layers were constrained at the bulk positions with optimized lattice constants of 4.028 Å, 3.977 Å, 3.994 Å and 3.925 Å (experimentally 3.912 Å[8]) for vdW−DF, PBE, BEEF−vdW and HSE06 respectively. The top three layers and the adsorbed CO molecules were fully optimized. An inter−slab spacing of 15 Å was used to minimize interactions between repeated slabs, together with dipole corrections.[9] The Brillouin zone of the $p(3\times3)$ and the $c(4\times2)$ unit cell was sampled with $(3\times3\times1)$ and $(3\times5\times1)$ Monkhorst−Pack grids, respectively. With these settings, adsorption energies were converged to within 3 kJ/mol. To evaluate the thermodynamic stability of the different structures, Gibbs free adsorption energies, ΔG_{ads} (300 K, 1 mbar), were obtained by combining the electronic and zero−point energies with enthalpy and entropy corrections from frequency calculations (Supporting Information Table S8) for the full structure. PBE frequencies were used to compute the Gibbs free adsorption energies for the HSE06 functional. Chemical bonding was analyzed using the periodic implementation of Natural Bond Orbitals (NBO) theory[10−11] and the Crystal Orbital Hamilton Population (COHP).[12−13] Bader charges were computed to evaluate the effect of charge.[14] Atom−projected density of states (PDOS) was obtained using the Lobster package.[13]

To confirm the relative change in CO adsorption energies of the top site and the bridge site to the surface platinum charge, calculations were performed on a 5−layer $p(3\times3)$ Pt(111) slab. The variation in the surface charge results from changes in the number of electrons in the 5−layer $p(3\times3)$ Pt(111) slab.
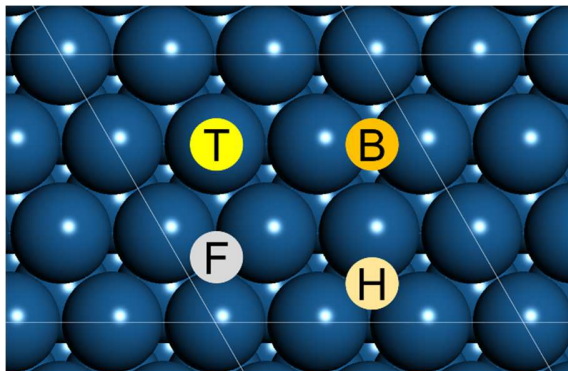
2. Figures

Figure S1. CO adsorption sites on a Pt(111) catalyst surface of a $p(3\times3)$ unit cell are shown: T−top, B−bridge, H−hollow−hcp and F−hollow−fcc
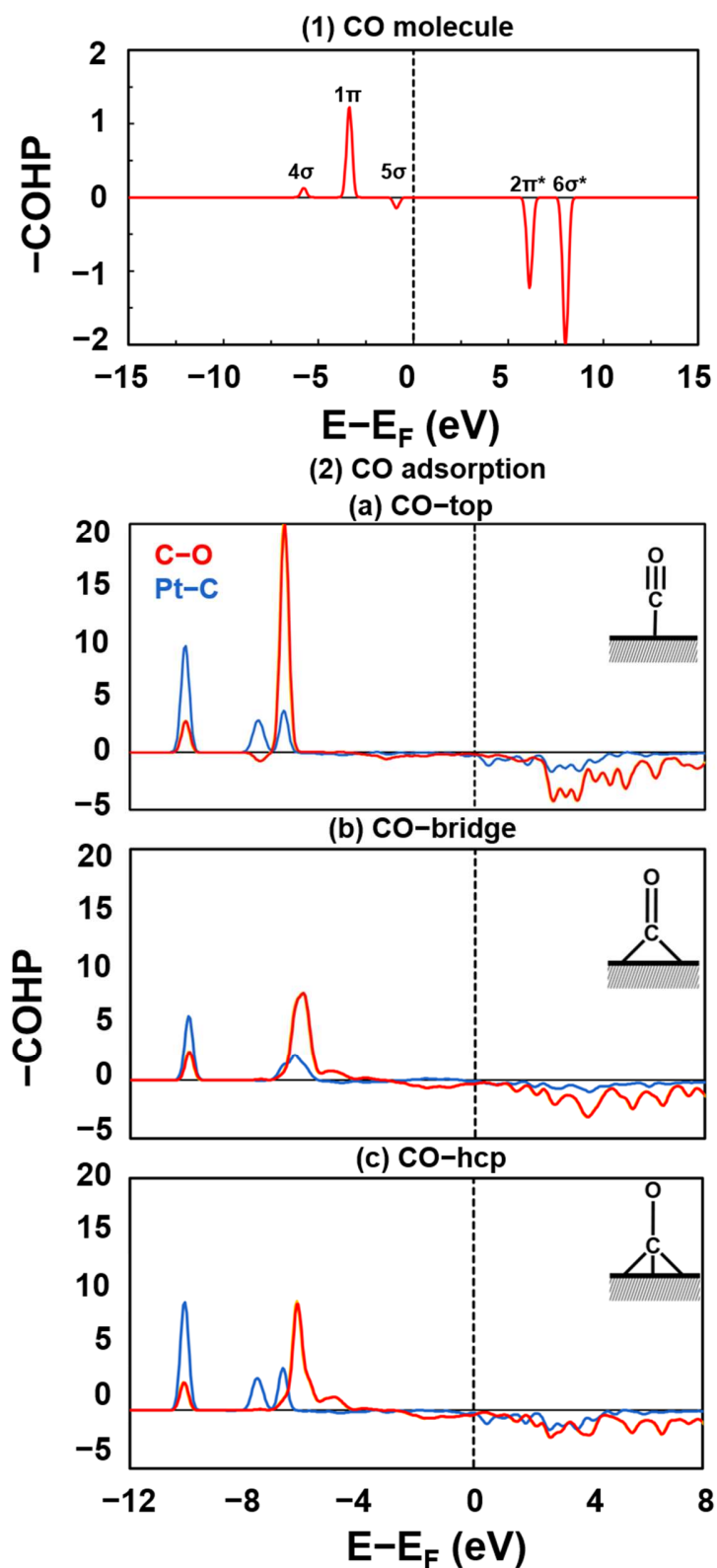
Figure S2. –COHP plots for (1) CO molecule in gas phase (2) CO adsorbed on a (a) top site (b) bridge site (c) hollow site for 1/9 ML CO coverage on the 5–layer $p(3{\times}3)$ Pt(111) slab.
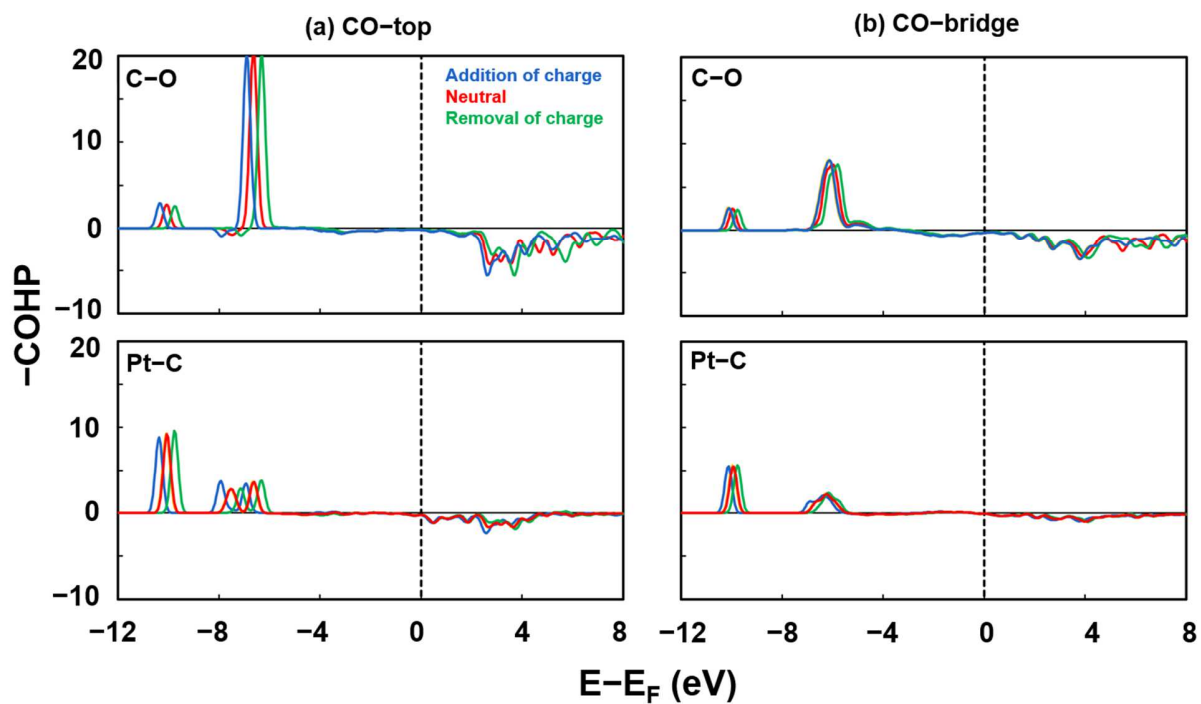
Figure S3. –COHP plots for CO adsorbed on a (a) top site (b) bridge site for 1/9 ML CO coverage on the 5–layer $p(3{\times}3)$ Pt(111) slab. The variation in the surface charge results from changes in the number of electrons in the Pt(111) slab.
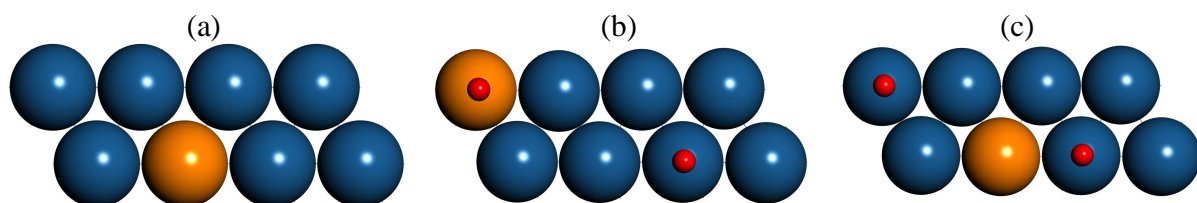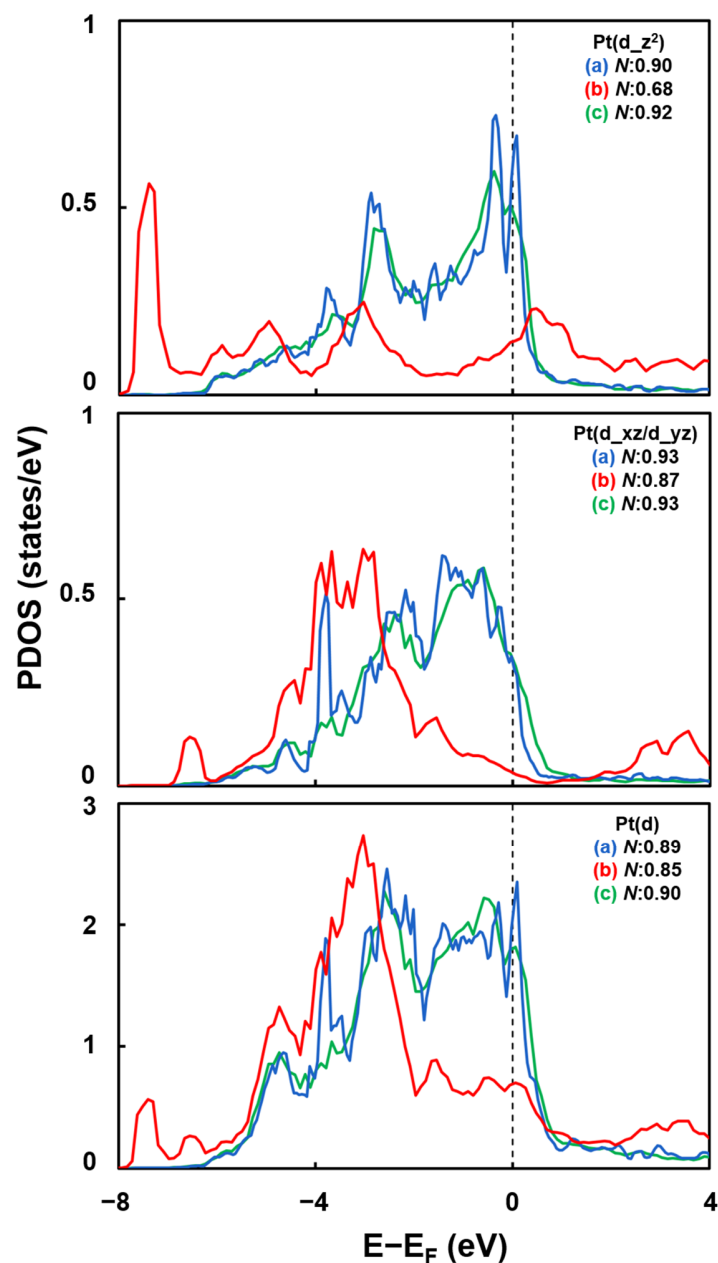
Figure S4. Atom−projected density of states (PDOS) for (a) a surface Pt atom in a clean $c(4\times2)$ unit cell (b) surface Pt atom where CO adsorbs, (c) empty surface Pt atom next to the Pt atom where CO is adsorbed (shown in orange). The filling of the d−states (N), calculated by integration of the density of states up to the Fermi level, is shown for the indicated Pt atom.
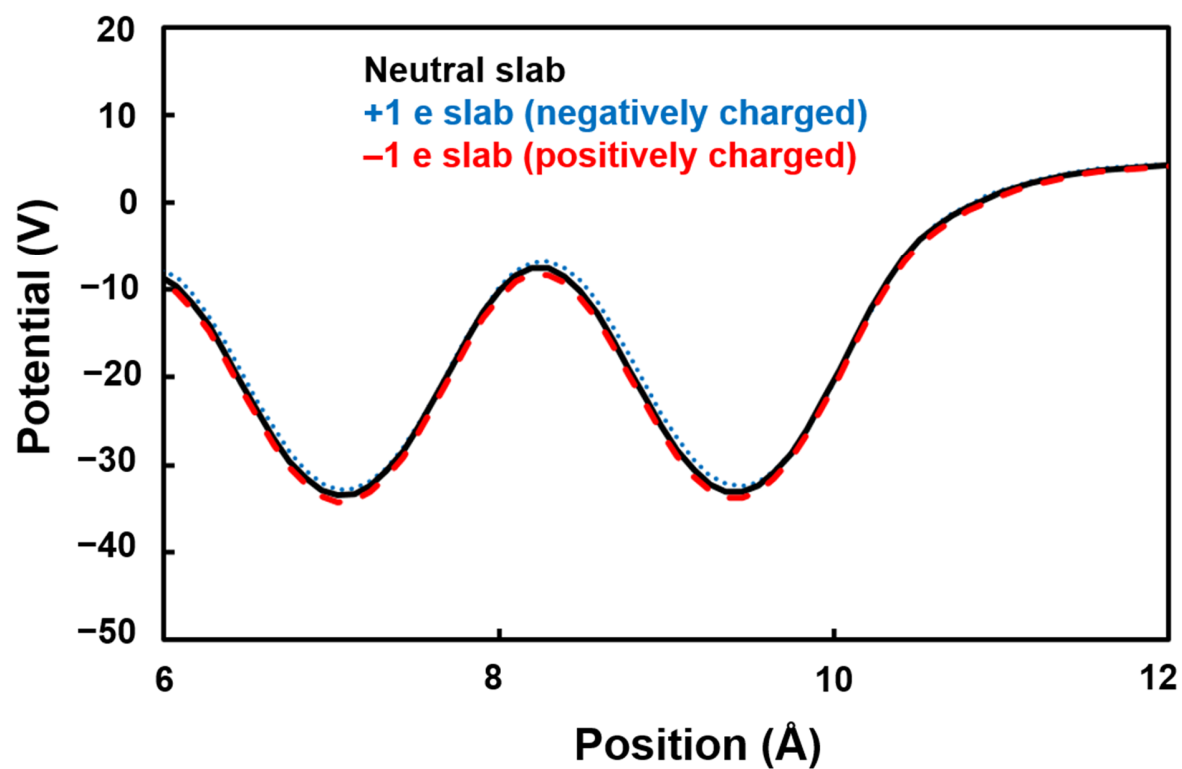
Figure S5. Planar averaged electrostatic potential along the normal axis for clean neutral and charged 5−layer *p*(3×3) Pt(111) slabs.
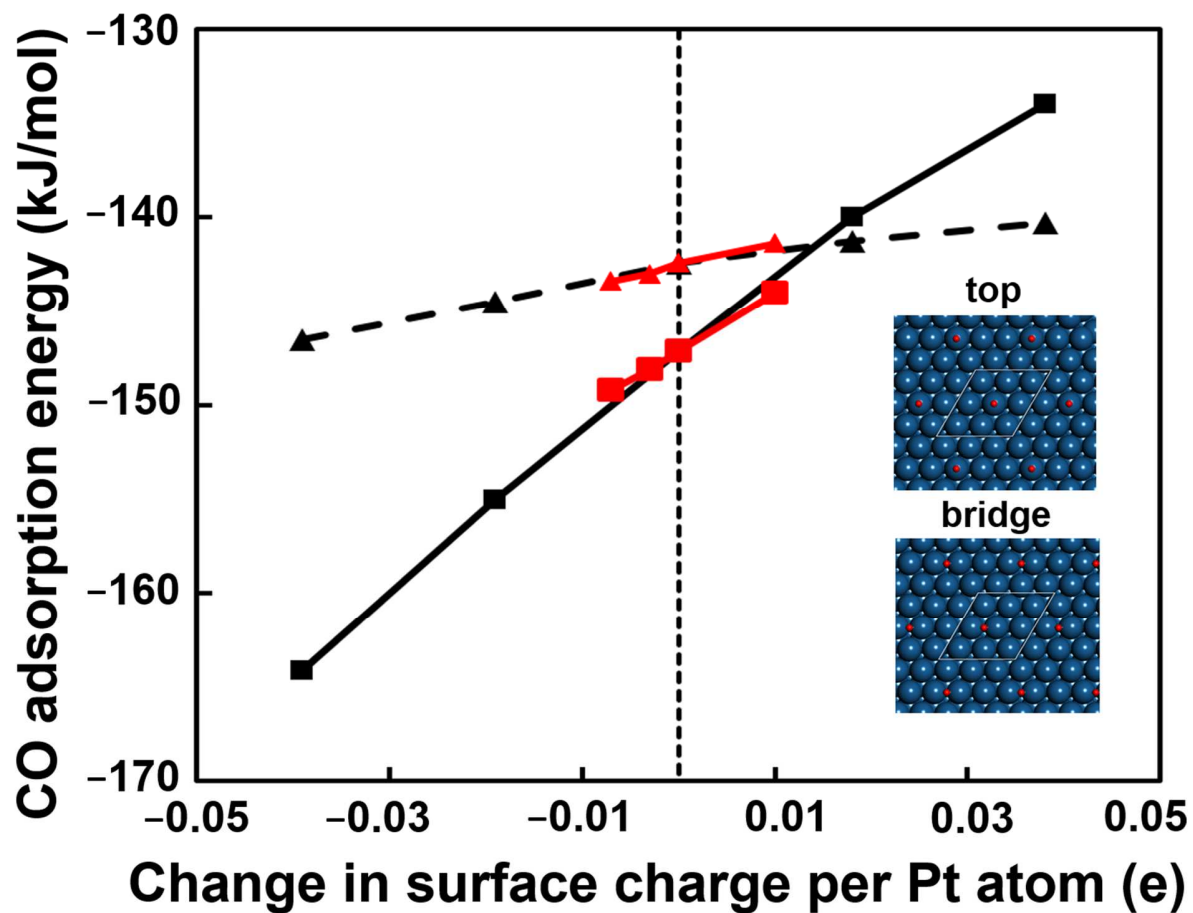
Figure S6. Effect of Pt charge on the CO adsorption energy for top (■) and bridge (▲) sites at 1/9 ML coverage. The variation in charge by adding/removing electrons to the slab is shown in black while variation in charge caused by the introduction of a homogeneous external field (0.2, 0.1, –0.1 V/Å) perpendicular to the surface is shown in red. In both cases, the change in adsorption energy correlates with the surface charge, even though the electrostatic field for a given charge is larger for the latter.

3. Tables

Table S1. CO adsorption energies (kJ/mol), Gibbs free adsorption energies (300 K, 1 mbar CO) (kJ/mol) and CO adsorption entropies (J/mol K) for different low coverage adsorption sites on Pt(111). The most stable adsorption site for each functional is indicated. (T–top, B–bridge, H–hollow)
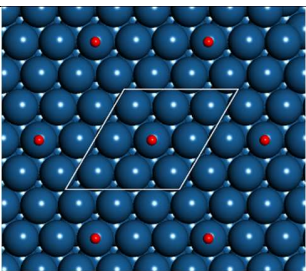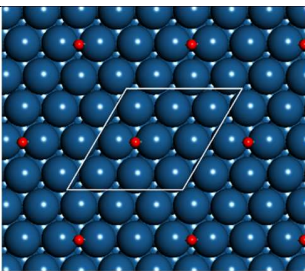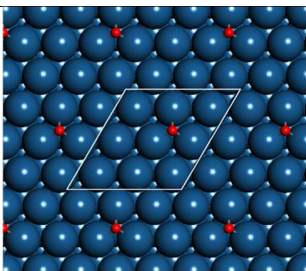
Functional	1/9 – 1T	1/9 – 1B	1/9 – 1H
vdW–DF	**−147**/−80/46	−143/−75/42	−139/−72/41
PBE	−174/−106/46	**−181**/−113/41	**−182**/−113/37
BEEF–vdW	−148/−80/47	**−152**/−84/41	−150/−82/39
HSE06	−199/−131/46	**−213**/−145/41	**−210**/−142/37

Table S2. C−O and Pt−C bond lengths (Å), CO stretch frequency (cm^{-1}), Lewis structure obtained from the NBO analysis, occupancy of the Pt−C σ* NBO, occupancy of the C−O π* NBO and change in charge of the CO molecule upon adsorption for low coverage CO structures on the 5−layer p(3×3) Pt(111) slab.

Coverage	1/9 − T	1/9 − B
d(C−O), d(Pt−C) (Å)	1.160, 1.850	1.184, 2.040, 2.040
CO stretch frequency (cm^{-1})	2021	1814
Lewis structure	O ‖‖‖ C │ Pt	O ‖ C ╱ ╲ Pt Pt
Pt−C σ* NBO occupancy (electrons)	0.511	0.470, 0.470
C−O π* NBO occupancy (electrons)	0.201, 0.201	0.220
Change in CO charge upon adsorption (electrons)	+0.030	+0.133

Table S3. Average CO adsorption energies (kJ/mol) for different low coverage configurations on a 5–layer Pt(111) slab with a $p(3\times3)$ unit cell obtained with optimized lattice constant of 4.028 Å and experimental lattice constant of 3.912 Å using vdW–DF functional. (T–top, B–bridge, H–hollow)
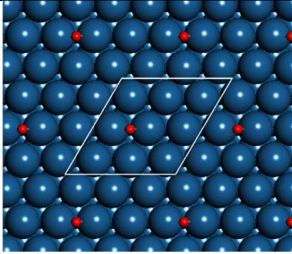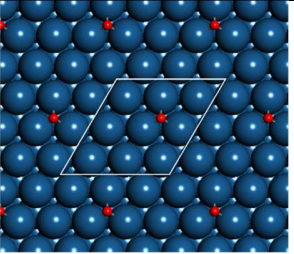
lattice constant	1/9 – 1T	1/9 – 1B	1/9 – 1H
Optimized	−147	−143	−139
Experimental	−145	−148	−143

Table S4. Average CO adsorption energies (kJ/mol), average Gibbs free adsorption energies (300 K, 1 mbar) (kJ/mol), and average CO adsorption entropies (J/mol K) for different high coverage structures in a $c(4\times2)$ unit cell obtained with vdW–DF and PBE functionals. The most stable configuration for each functional is shown in bold. (T–top, B–bridge).
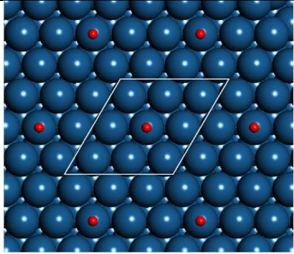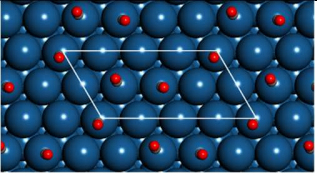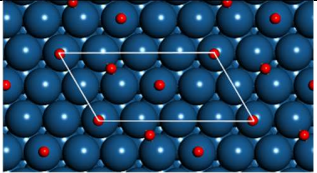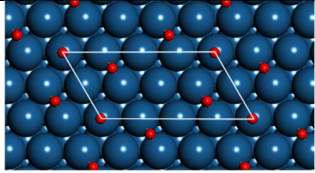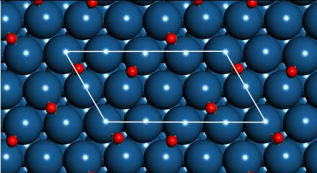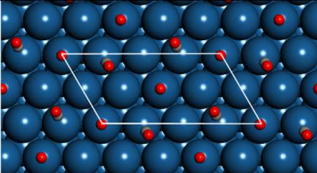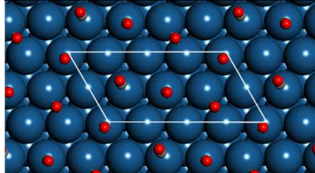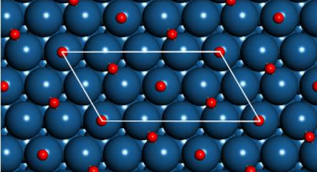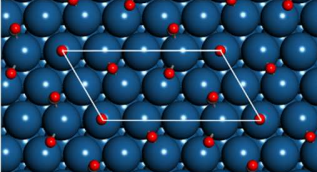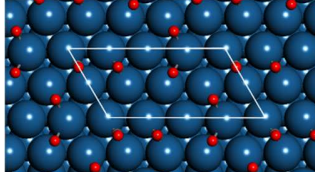

	3/8 – 3T	3/8 – 2T+1B	3/8 – 1T+2B
vdW–DF	−135/−68/49	**−141**/−73/45	−138/−70/43
PBE	−161/−92/46	−169/−100/44	**−171**/−101/41

	3/8 – 3B	1/2 – 4T	1/2 – 3T+1B
vdW–DF	−133/−64/41	−127/−60/49	−135/−67/46
PBE	−168/−99/39	−158/−89/47	−161/−92/44

	1/2 – 2T+2B	1/2 – 1T+3B	1/2 – 4B
vdW–DF	**−139**/−70/43	−132/−63/42	−122/−53/40
PBE	**−168**/−98/41	−165/−95/39	−163/−94/38

14

Table S5. Low coverage vdW−DF CO adsorption energy as the charge of the surface Pt atoms changes in the 5−layer $p(3\times3)$ Pt(111) slab. The neutral slab corresponds to a negative charge of 0.047 e/Pt.

Surface charge per Pt (e)	CO adsorption energy (kJ/mol)	
	top site	bridge site
0.008	−164	−147
0.028	−155	−144
0.047 (Neutral slab)	−147	−142
0.065	−140	−141
0.085	−134	−140

Table S6. Change in the occupancy of various NBOs for CO adsorption at the top and the bridge site as a function of the charge of the surface Pt atoms. Calculations were done for a low CO coverage, with the vdW–DF functional and for a 5–layer $p(3{\times}3)$ Pt(111) slab. The neutral slab corresponds to a negative surface Pt charge of 0.047 e/Pt.

	NBO Occupancy (electrons)					
	Top site			Bridge site		
	0.008 (positively charged)	0.047 (Neutral)	0.085 (negatively charged)	0.008 (positively charged)	0.047 (Neutral)	0.085 (negatively charged)
Pt–C σ	1.975	1.975	1.975	1.764 (2)	1.764 (2)	1.764 (2)
Pt–C σ*	**0.501**	**0.511**	**0.521**	**0.465** (2)	**0.470** (2)	**0.476** (2)
C–O σ	1.986	1.986	1.986	1.984	1.984	1.984
C–O σ*	0.008	0.009	0.010	0.012	0.017	0.021
C–O π	1.989 (2)	1.989 (2)	1.989 (2)	1.982	1.982	1.982
C–O π*	**0.171** (2)	**0.201** (2)	**0.221** (2)	**0.195**	**0.220**	**0.250**
O L.P.	1.962	1.962	1.962	1.950	1.950	1.950

Table S7. Effect of the surface Pt charge on the low coverage CO adsorption energy for the PBE functional and a 5–layer $p(3\times3)$ Pt(111) slab. The neutral slab corresponds to a negative surface Pt charge of 0.045 e/Pt.

Surface charge per Pt (e)	CO adsorption energy (kJ/mol)	
	top site	bridge site
0.009	−188	−183
0.045 (Neutral slab)	−174	−181
0.083	−160	−179

Table S8. vdW−DF frequencies of adsorbed CO for different configurations and coverages on Pt(111). (T–top, B–bridge, H–hollow)

CO adsorption configuration	Frequencies [cm^{-1}]
p(3×3) unit cell	
1/9 – T	2021, 456, 382, 381, 78, 70
1/9 – B	1814, 369, 364, 353, 195, 58
1/9 – H	1725, 314, 288, 287, 149, 146
c(4×2) unit cell	
3/8 – 3T	2027, 1995, 1983, 449, 443, 443, 393, 383, 375, 371, 368, 357, 85, 77, 61, 59, 56, 51
3/8 – 2T+1B	2030, 2010, 1797, 448, 443, 391, 384, 382, 382, 377, 375, 354, 189, 76, 69, 65, 64, 64
3/8 – 1T+2B	2030, 1819, 1802, 440, 395, 387, 372, 369, 368, 366, 350, 347, 196, 191, 74, 71, 62, 57
3/8 – 3B	1852, 1819, 1810, 379, 370, 367, 360, 358, 344, 340, 326, 325, 192, 190, 187, 93, 70, 61
1/2 – 4T	2030, 1990, 1976, 1969, 446, 442, 435, 432, 410, 406, 376, 374, 371, 363, 309, 301, 106, 103, 76, 67, 60, 52, 44, 43
1/2 – 3T+1B	2033, 2005, 1984, 1796, 445, 442, 436, 402, 397, 390, 381, 377, 377, 374, 350, 345, 196, 95, 88, 71 ,65, 62, 62, 50
1/2 – 2T+2B	2037, 2018, 1806, 1792, 443, 442, 400, 391, 388, 387, 386, 377, 375, 374, 351, 350, 194, 190, 82, 77, 74, 74, 66, 63
1/2 – 1T+3B	2033, 1866, 1814, 1809, 454, 440, 407, 395, 388, 377, 372, 368, 366, 346, 323, 276, 205, 191, 159, 88, 77, 72, 69, 67
1/2 – 4B	1892, 1840, 1823, 1800, 460, 406, 394, 387, 374, 366, 362, 334, 327, 298, 289, 264, 216, 185, 180, 146, 130, 93, 89, 64
1 – 8T	2075, 1998, 1997, 1965, 1964, 1964, 1964, 1963, 462, 460, 456, 447, 447, 438, 437, 433, 423, 423, 413, 412, 411, 410, 410, 409, 408, 407, 404, 401,

401, 395, 395, 394, 276, 272, 271, 251, 251, 215, 215, 207, 206, 169, 165, 164, 132, 132, 85, 78

1 – 8B   1971, 1896, 1896, 1861, 1858, 1858, 1856, 1855, 570, 569, 521, 507, 507, 483, 483, 461, 460, 423, 423, 413, 413, 411, 392, 369, 360, 346, 329, 328, 320, 320, 311, 308, 307, 307, 280, 280, 272, 264, 263, 232, 232, 227, 180, 178, 171, 148, 147, 87

4. References

(1) Dion, M.; Rydberg, H.; Schröder, E.; Langreth, D. C.; Lundqvist, B. I. Van der Waals density functional for general geometries. *Phys. Rev. Lett.* 2004, 92, 246401.

(2) Klimeš, J.; Bowler, D. R.; Michaelides, A. Van der Waals density functionals applied to solids. *Phys. Rev. B* 2011, 83, 195131.

(3) Perdew, J. P.; Burke, K.; Ernzerhof, M. Generalized Gradient Approximation Made Simple. *Phys. Rev. Lett.* 1996, 77, 3865.

(4) Wellendorff, J.; Lundgaard, K. T.; Møgelhøj, A.; Petzold, V.; Landis, D. D.; Nørskov, J. K.; Bligaard, T.; Jacobsen, K. W. Density functionals for surface science: Exchange−correlation model development with Bayesian error estimation. *Phys. Rev. B* 2012, 85, 235149.

(5) Krukau, A. V.; Vydrov, O. A.; Izmaylov, A. F.; Scuseria, G. E. Influence of the exchange screening parameter on the performance of screened hybrid functionals. *J. Chem. Phys.* 2006, 125, 224106.

(6) Kresse, G.; Furthmüller, J. Efficient iterative schemes for ab initio total−energy calculations using a plane−wave basis set. *Phys. Rev. B: − Condens. Matter* 1996, 54, 11169.

(7) Kresse, G.; Furthmüller, J. Efficiency of ab−initio total energy calculations for metals and semiconductors using a plane−wave basis set. *Comput. Mater. Sci.* 1996, 6, 15.

(8) Wyckoff, R. W. G., *Crystal Structures*. Krieger Publishing: Malabar FL, 1982; Vol. 1.

(9) Makov, G.; Payne, M. C. Periodic boundary conditions in ab initio calculations. *Phys. Rev. B* 1995, 51, 4014−4022.

(10) Dunnington, B. D.; Schmidt, J. R. Generalization of Natural Bond Orbital Analysis to Periodic Systems: Applications to Solids and Surfaces via Plane−Wave Density Functional Theory. *J. Chem. Theory Comput.* 2012, 8, 1902−1911.

(11) Weinhold, F.; Landis, C. In *Valency and Bonding − A Natural Bond Orbital Donor−Acceptor Perspective*, Cambridge University Press: Cambridge, 2005; pp 1−44.

(12) Dronskowski, R.; Bloechl, P. E. Crystal orbital Hamilton populations (COHP): energy−resolved visualization of chemical bonding in solids based on density−functional calculations. *J. Phys. Chem.* 1993, 97, 8617−8624.

(13) Deringer, V. L.; Tchougréeff, A. L.; Dronskowski, R. Crystal Orbital Hamilton Population (COHP) Analysis As Projected from Plane−Wave Basis Sets. *J. Phys. Chem. A* 2011, 115, 5461−5466.

(14) Bader, R. F. W. In *International Series of Monographs on Chemistry*, Oxford University Press: Oxford, 1990; Vol. 22, pp 5−6.